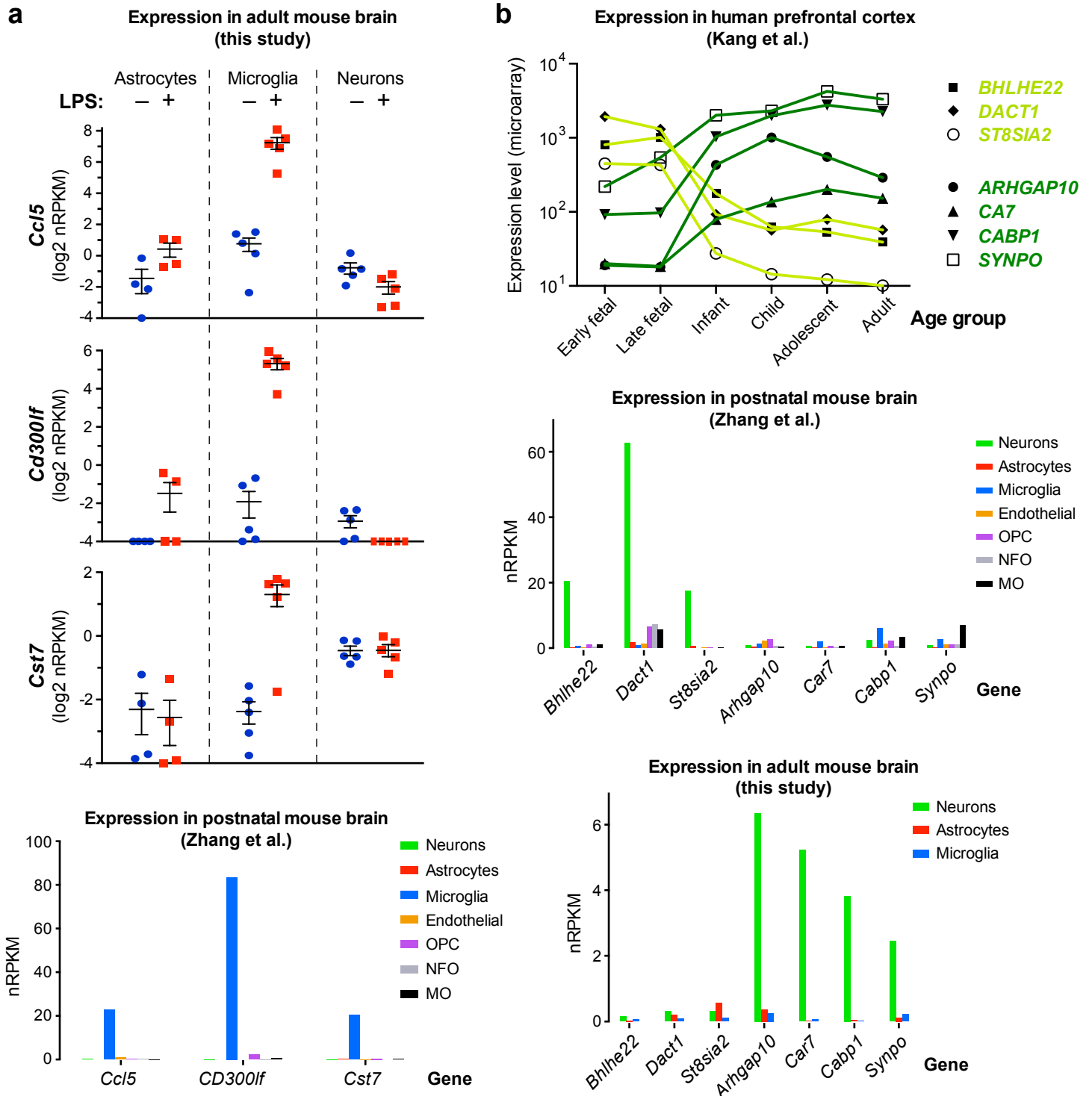
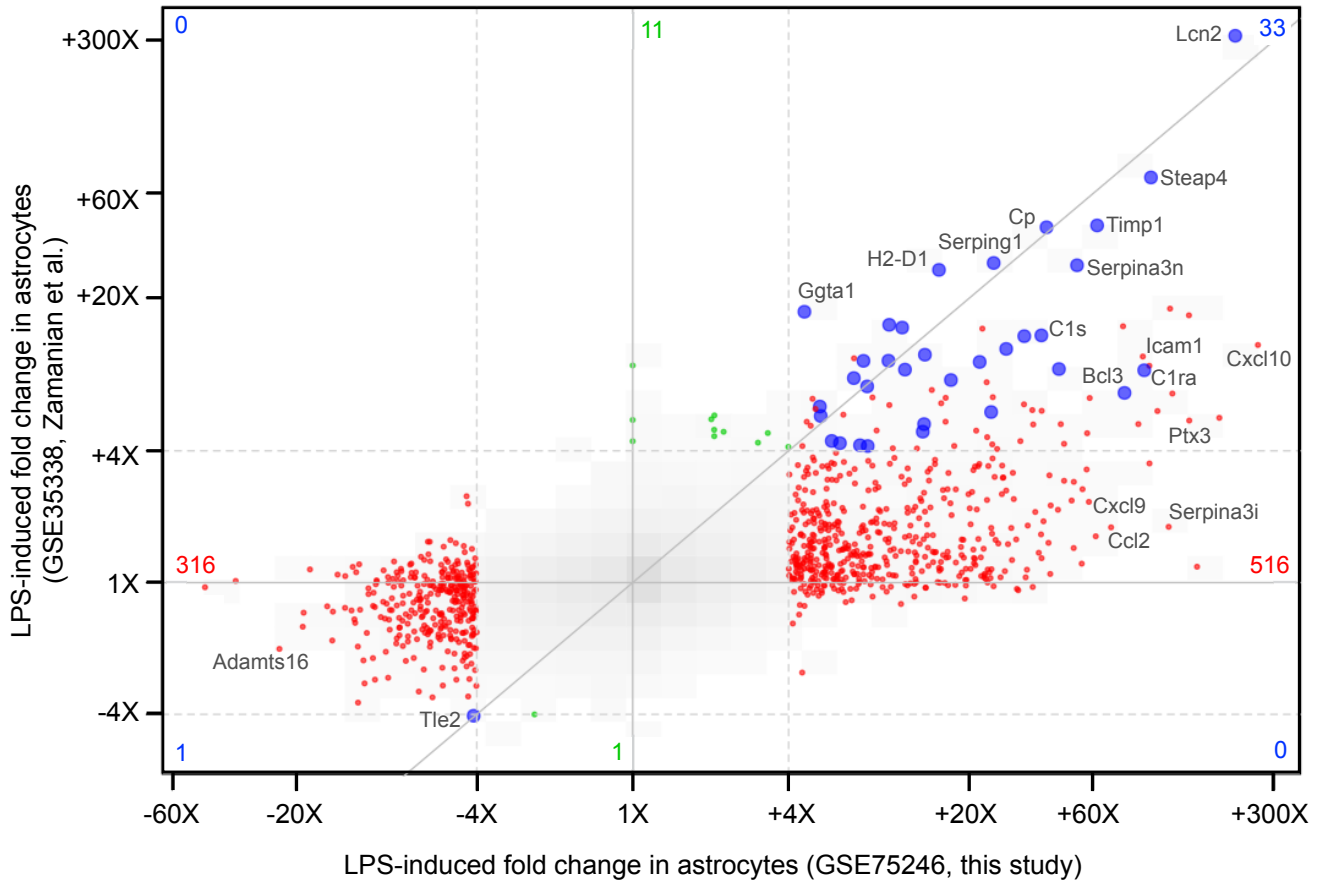


Supplementary Figure 1 | Cell type marker expression in FACS-isolated cells from adult mouse cortex (qPCR).
(a) RNA from cells isolated using anti-NeuN (*Rbfox3*, neurons), anti-GFAP (astrocytes), or anti-CD11b (*Itgam*, microglia) was tested by RT-qPCR for expression of the same markers used for sorting. Markers were normalized to *Gapdh* expression, and bars represent mean \pm s.d. (Prism). **(b)** Additional markers expressed by neurons (top row), astrocytes (middle row), and microglia (bottom row) were tested by RT-qPCR for expression level in NeuN⁺, GFAP⁺, and CD11b⁺ sorted cell populations.

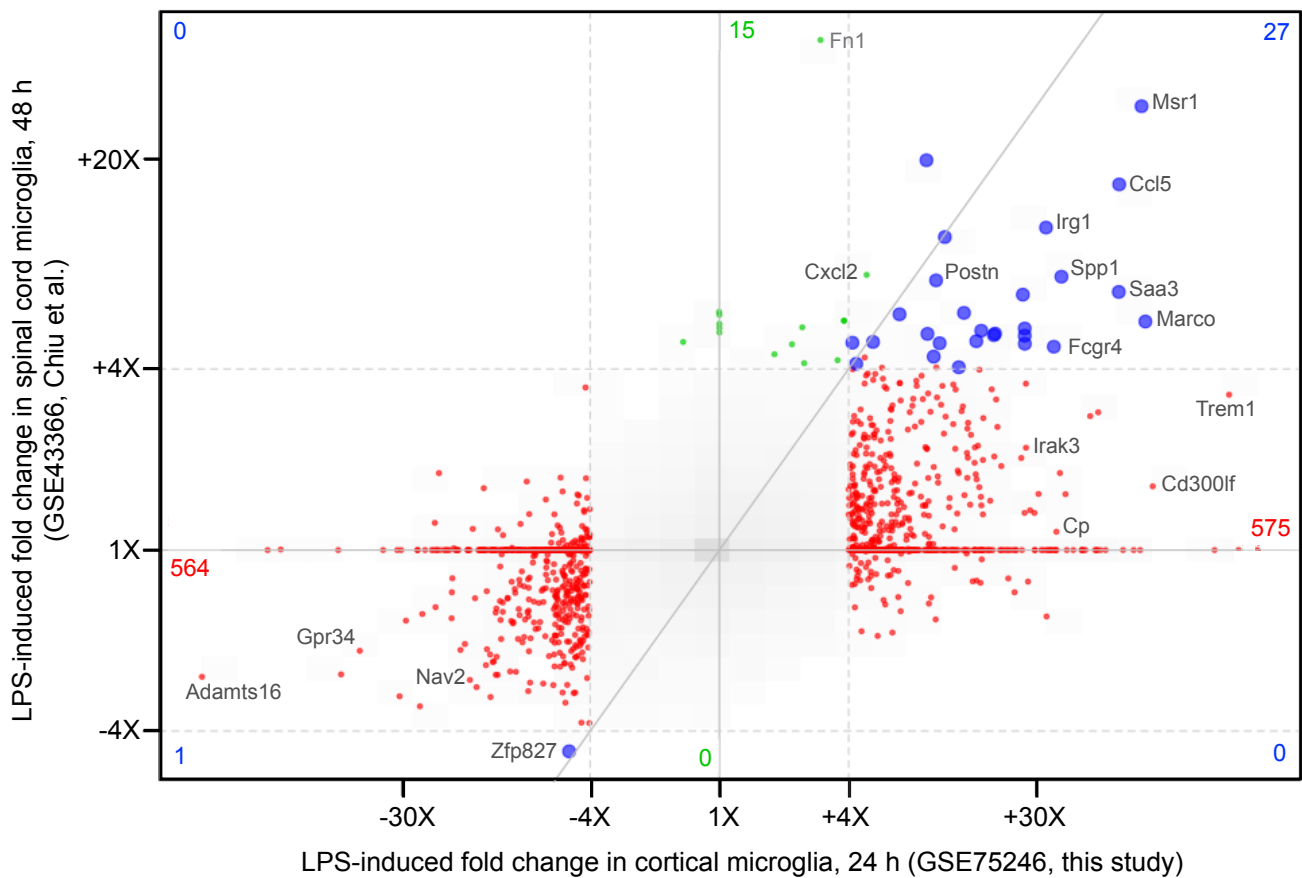


Supplementary Figure 2 | Our method yields expression profiles for microglia and neurons in their unperturbed, mature states. (a) Certain genes reported by others (Zhang et al., GSE52564) to be highly expressed in microglia (median values plotted, $n=2$ per cell type) were not observed in our data (GSE75246) unless the animals were somehow challenged as with LPS injection ($n=4-5$ samples per cell type plotted individually, bars = mean \pm s.e.m. (Prism)). (b) Certain genes expressed in postnatal (GSE52564, $n=2$ per cell type) but not adult (GSE75246, $n=4-5$ per cell type) mouse neurons were robustly detected in fetal but not adult human prefrontal cortex (Kang et al., GSE25219). Conversely, certain genes expressed in adult but not postnatal mouse neurons were expressed more highly in adult than fetal human prefrontal cortex. Median values plotted. Early fetal = 8-17 weeks post-conception ($n=88$ tissue specimens), late fetal = 19-37 weeks post-conception ($n=64$), infant = < 1 year after birth ($n=28$), child = 1-9 years ($n=32$), adolescent = 11-19 years ($n=28$), and adult = 21-64 years ($n=91$). *Note: nRPKM values cannot be directly compared between GSE52564 and GSE75246 due to different library preparation methods. However, relative nRPKM differences among cell types within a study should be comparable between studies.



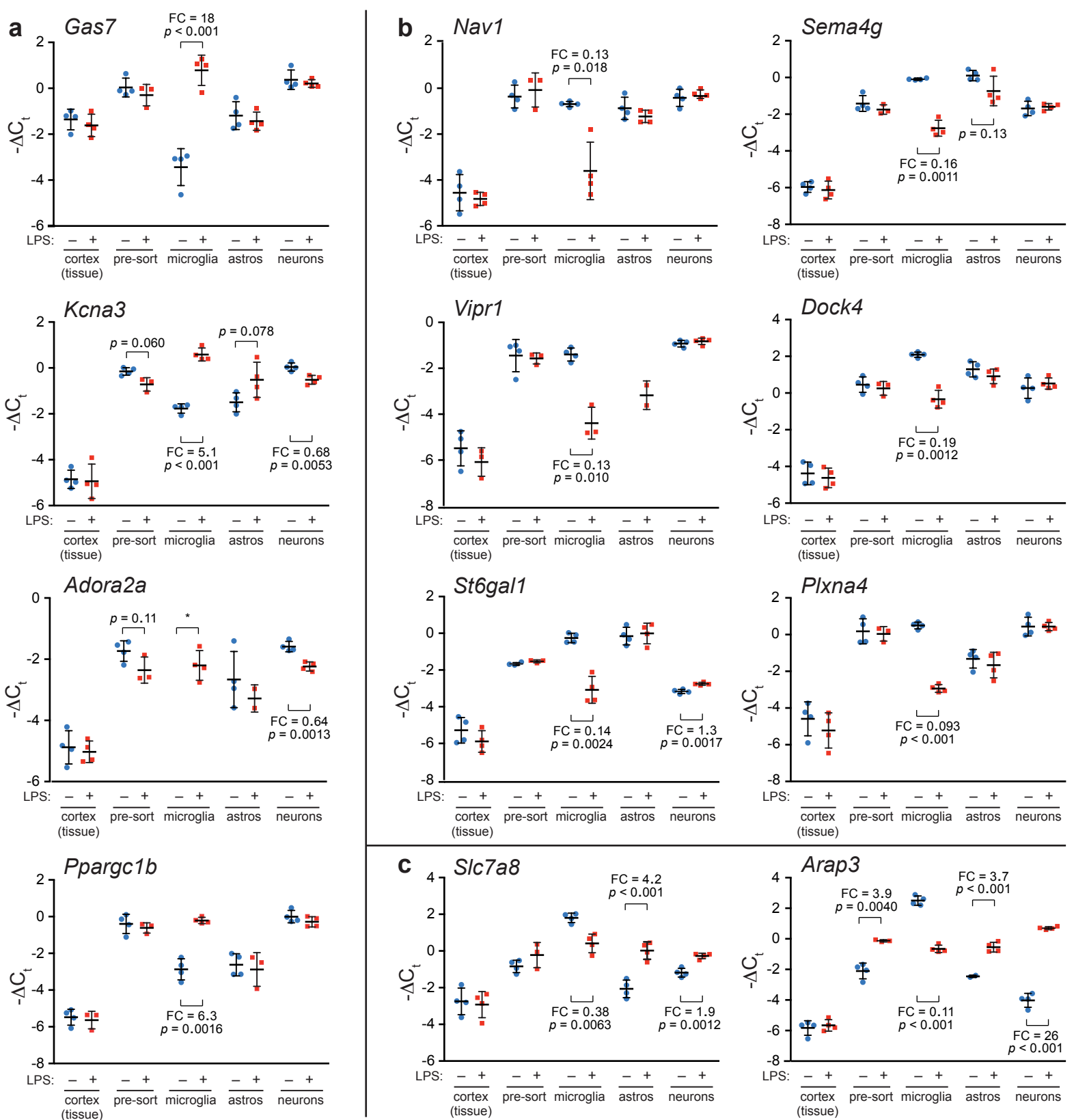
Supplementary Figure 3 | Comparison of expression profiles for astrocytic response to endotoxemia.

This genome-wide "4-way" plot compares LPS-induced changes in astrocytic gene expression in this study (GSE75246) with those reported previously (GSE35338, Zamanian et al.). Each point represents a gene with ≥ 4 -fold change (adjusted $p \leq 0.05$) in either study, with the fold-change between astrocytes from LPS-injected vs. control mice in our study plotted on the x-axis and that from GSE35338 on the y-axis. Blue points meet the cutoffs in both studies, red points only in our study, and green points only in GSE35338. The gray color indicates the distribution of fold-change values for all genes. (Genes for which no microarray data were available in GSE35338 are not plotted.) Possible reasons for the increased detection of LPS-induced genes in our study include the sensitivity of RNA sequencing compared to microarrays, the dose and strain of LPS used, and different methods for dissociating, labeling, and purifying astrocytes from intact mouse brain. See Supplementary Data 2 for interactive report of LPS-induced genes in our study.

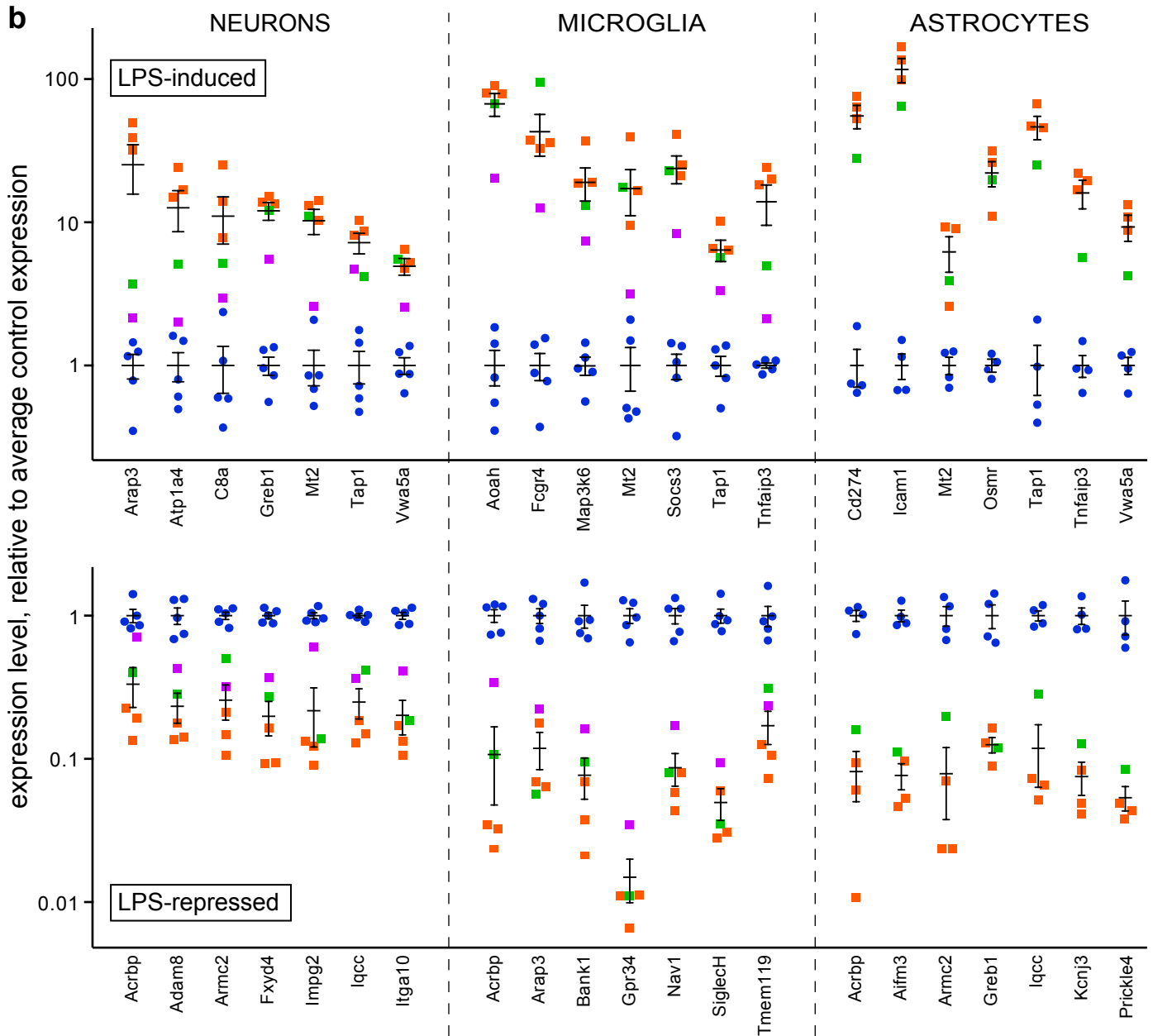
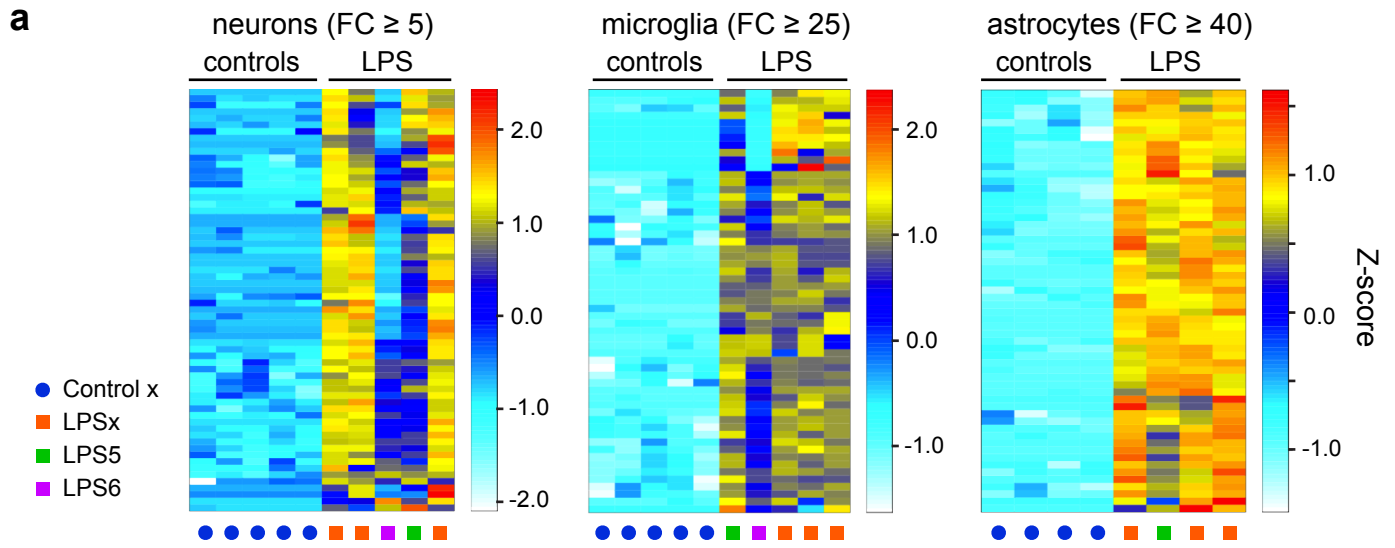


Supplementary Figure 4 | Comparison of expression profiles for microglial response to endotoxemia.

This genome-wide "4-way" plot compares LPS-induced changes in microglial gene expression in this study (GSE75246) with those reported previously (GSE43366, Chiu et al.). Each point represents a gene with ≥ 4 -fold change (adjusted $p \leq 0.05$) in either study, with the fold-change between microglia from LPS-injected vs. control mice in our study plotted on the x-axis and that from GSE43366 on the y-axis. Blue points meet the cutoffs in both studies, red points only in our study, and green points only in GSE43366. The gray color indicates the distribution of fold-change values for all genes. Possible reasons for the increased detection of LPS-induced genes in our study measuring the transcriptional response at an earlier time point post-injection, the dose and strain of LPS used, the larger sample size in our study, differences between brain and spinal cord, and the different methods for dissociating and purifying microglia from intact CNS tissue. See Supplementary Data 2 for interactive report of LPS-induced genes in our study.



Supplementary Figure 5 | Our method allows detection of differentially expressed genes in purified cell types that cannot be detected using whole tissue RNA samples. 24 h after peripheral injections with LPS or saline (n=4/group), perfused mouse brains were processed using one cortical hemisphere for whole tissue RNA and the other for dissociating and purifying individual cell types, followed by RT-qPCR tests for LPS-induced changes. Genes such as *Gas7*, *Kcna3*, *Adora2a*, and *Ppargc1b* were upregulated (a) in microglia from LPS-injected mice, while genes such as *Nav1*, *Vipr1*, *St6gal1*, *Sema4g*, *Dock4*, and *Plxna4* were downregulated (b). These changes were not observed in RNA from whole tissue or from dissociated, DAPI⁺ cells (“pre-sort”) due to constitutive expression in other CNS cell types. *Slc7a8* and *Arap3* were LPS-induced in astrocytes and neurons, but these changes were not observed in whole tissue RNA due to offsetting decreases in microglial expression (c). Bars represent mean \pm s.d., with fold change (FC) and unadjusted p-values (two-tailed t-test, unequal variance, unadjusted) shown. C_t values were normalized against *Gapdh* and *Hprt*. Note: For sorted cells, the fixation step affects RNA recovery for each gene differently, but consistently across samples for a given gene. Thus, although $-\Delta C_t$ values from whole brain (unfixed) are frequently different than pre-sort (fixed), $\Delta\Delta C_t$ values (fold changes) are preserved when comparing across treatments or disease states. Data points and calculations for fold change and p-value are absent when the target gene was undetected. One LPS “pre-sort” sample failed to amplify in all assays.



Supplementary Figure 6 | Overall LPS response is consistent between cell types of a single animal.

(a) For each cell type, a short list of the top ~60 LPS-induced genes was selected at $p \leq 0.05$ and the indicated fold-change (FC). Heat maps show the Z-score-normalized $\log_2(\text{nRPKMs})$ for these genes (rows) within the corresponding cell types, with each column representing that cell type from a single animal injected with either saline (blue dots) or LPS (colored squares). The LPS6 animal (magenta square) consistently showed a very weak transcriptional response in both neurons and microglia. (The astrocytes from this animal were excluded from the study due to neuronal contamination.) The LPS5 animal (green square) was also somewhat attenuated relative to the remaining three LPS-injected animals (orange squares). (b) Examples of LPS-induced (top chart) and LPS-repressed (bottom chart) gene expression from RNA-Seq data in each cell type demonstrate the overall trend that the transcriptional response in the LPS6 animal was severely attenuated in multiple cell types, and the response in the LPS5 animal was, overall, modestly attenuated in each cell type. Bars represent mean \pm s.e.m. (Prism).

